Case Study on Causes and Countermeasures of a Largely Deformed Reinforced Earth Wall with Geotextile in Hyogo, Japan



Satoru Shibuya
Professor, Department of Civil Engineering, Kobe University, Japan

Jinsuk Hur & Minsu Jung
Department of Civil Engineering, Kobe University, Japan & Korea Institute of Construction Technology, Korea

ABSTRACT: This study examines causes and countermeasures of large deformation that took place on the reinforced earth wall, a part of the Tottori expressway planned to pass Hyogo, Japan. Since this reinforced earth wall had experienced unexpected deformation of the wall during construction, the wall was re-constructed twice. However, the wall deformation showed no sign to cease even at the final stage of the construction. In this paper, case study was carried out on the interpretation of the mechanical behavior of the severely damaged reinforced earth wall comprising geotextile with the concrete panel facing. At First, the outline of the damaged reinforced earth wall is in detail described. The background and cause of the damage are discussed based on the results of site investigation. The engineering properties of the fill were examined by performing various in-situ and laboratory tests, including the surface wave survey (SWS), PS-logging, RI-logging, soaking test, the direct shear box (DSB) test, bender element (BE) test, etc. Consequently, the background as well as the cause for the damage of the wall may be described such that i) a considerable amount of settlement took place over a 3m thick weak soil layer in the lower part of the reinforced earth due to seepage of rainfall water, ii) the weight of the upper fill was partially supported by the geo-textile hooked on the concrete panels (n.b., named conveniently “hammock state” in this paper), and iii) the concrete panels to form the hammock were severely damaged by the unexpectedly large downwards compression force triggered by the tension force of the geotextile. And then, numerical analysis was carried out in order to simulate the development of the large deformation that took place on the reinforced earth wall and countermeasures to re-stabilize the wall were demanded. As the results of site investigation, it was manifested that subsidence of a 3-meter weak soil due to seepage flow was responsible for the large deformation. A part of concrete panel wall was severely damaged due to extremely large pulling force of geotextile induced by the hammock state. As for the countermeasures, “grouting with slag system” was applied to fill voids of the backfill, and also to prevent further development of settlement in the weak soil layer. “Ground anchor” was also considered to achieve the prescribed factor of safety.

1 INTRODUCTION

An interpretation of the mechanical behavior of a severely damaged reinforced earth wall comprising geotextile with the concrete panel facing was carried out. The background and cause of the damage are discussed based on the results of site investigation. The engineering properties of the fill were examined by performing various in-situ and laboratory tests, including the HR-SW survey, PS-logging, RI-logging, soaking test, the direct shear box test, bender element (BE) test, *etc*.

In Japan, reinforced earth wall with geotextile is popular for the construction of roads in mountain area. The use of reinforced earth comprising the vertical or very steep facing is advantageous in terms of the construction cost when compared to bridges, for example. In the case of reinforced

earth wall comprising geotextile with the concrete panel facing, however, it involves a great difficulty in compacting properly the portion of the fill adjacent to the wall facing. As a result of loose compaction near the wall, the wall facing may be damaged by compressive force and/or could be completely destroyed due to the active failure of the fill (for example, refer to Tatsuoka.et al., 1997).

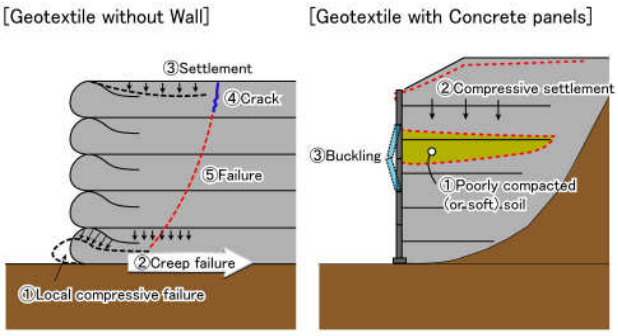

Fig. 1 Typical damages of reinforced earth walls.

Fig. 1 shows typical of damages for reinforced earth in general. In case of flexible reinforced earth without any concrete facing, a local failure involving with excessive compressive deformation would take place at the bottom portion, which in turn may trigger the overall active slip failure in a progressive manner (refer to Tatsuoka et al., 2000).

Conversely, when the reinforced earth with concrete panels comprises a poorly compacted (or soft soil) layer at the time of construction, a connection between the concrete panel and reinforcement member (i.e., the metal strip or geotextile) would be destroyed owing to the downward tension force at the connection, which eventually may bring about complete failure of the wall. Case study described in this sub-section refers to the latter case.

Fig. 2 Location of the site.

As seen in Fig.2, the severely-damaged reinforced earth wall with 150m long and the maximum height of 15m is situated at the end of the newly constructed Tottori expressway. It is bounded by valleys in the mountain area in Hyogo Prefecture, Japan. The wall is a reinforced earth wall with geo-textile constructed using fine-grained local soils.

The details of the wall are shown in Fig. 3. In November of 2006, irregular deformation of the wall was observed at the middle stage of the construction. Accordingly, a partial reconstruction involved with cement stabilization to the fill was carried out after removing some parts of the reinforced earth wall, which is called “the first remedy” in this paper.

In April of 2007, unexpected deformation of the

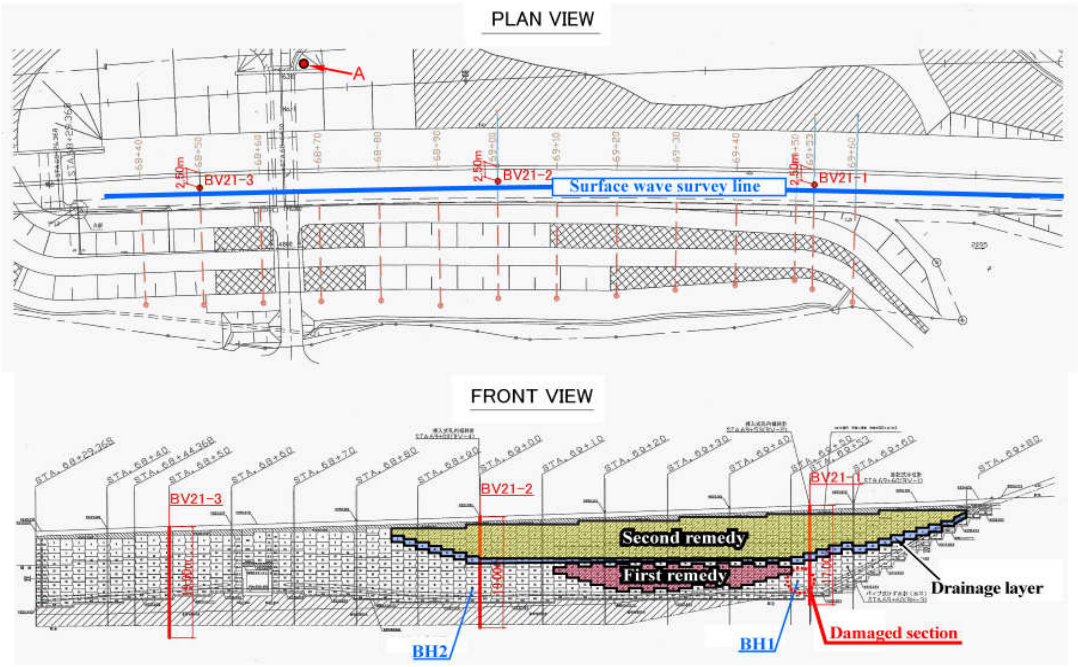

Fig. 3 Front and plan views of the site.

wall was again observed at the eleventh stage of the construction being close to the final construction stage. Therefore, after demolishing some parts of the wall, the wall was reconstructed with cement stabilization to the upper part of the fill. Furthermore, a horizontal drainage layer was installed in the middle part of the wall. In this paper, this reconstruction of the wall is called "the second remedy" (refer to Fig.15). The locations for HR-SW survey, PS-logging, RI-logging, boring and the SPT are indicated in Fig.3.

The wall height at the severely damaged portion was approximately 15m. As described earlier, the parts of the fill for the first and second remedies had been improved by cement injection using the dry weight of Portland cement of 50kg/m^3.

The drainage layer was sandwiched between these two cement-mixed layers. Note that the severely damaged portion of the wall is surrounded by the improved soil with a low-permeability and the bedrock. In addition, there is a small valley behind it.

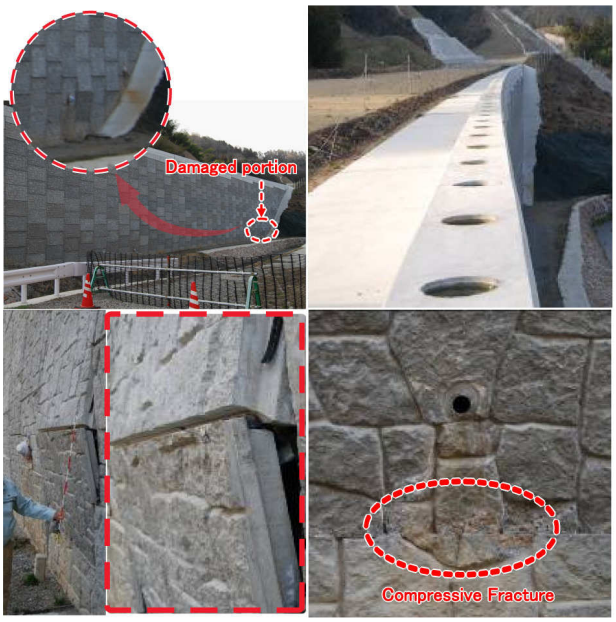

Fig. 4 Severely damaged portion.

The construction of the wall was finally completed in November, 2007. However, the field observation clearly indicated that the deformation of the wall showed no tendency to stabilize with time. Case study was hence commissioned in order to manifest the cause of the wall damage, and also to examine effective counter-measures to re-stabilize the wall. Fig. 4 shows some pictures of the reinforced earth wall cited, including the severely damaged portion. The outwards deformation at the damaged portion on the wall was on-going by showing the horizontal displacement to reach the value as large as 166mm. The concrete panel wall had been constructed by using a high-density polythene geo-textile sheet. Based on the observation, a type of wall damage due to the existence of a poorly compacted soil layer was strongly suspected (refer to Fig. 1).

2 IN-SITU AND LABORATORY TESTS

The HR-SW survey was carried out to figure out the 2D profile of the elastic wave velocities, i.e., S-wave and P-wave velocities (Vs and Vp) of the fill, together with the foundation. Fig. 5 shows the profiles of Vs and Vp with depth for the 160m long survey line L1. In general, the Vs increases with depth involved with increase in in-situ stresses.

However, a low-velocity layer was observed for Vs near the severely damaged section at BV21-1 (n.b., elevation: approximately 240m, distance: 110~115m). The decrease in Vs strongly suggests some reduction of the magnitude of stresses at the deformed section.

On the other hand, the dashed curve in the profile of V_p represents the boundary associated with V_p = 1500m/s, noting that the specific condition of V_p = 1500m/s is applicable to saturated condition. Accordingly, it may be surmised that the state of soil behind the damaged panels is close to saturation.

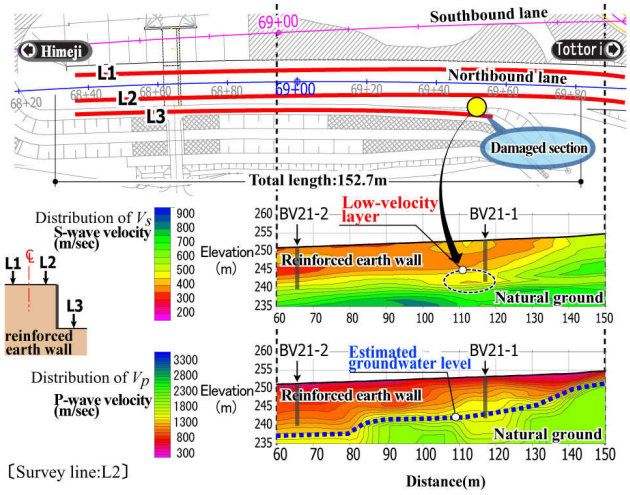

Fig. 5 Results of HR-SW survey.

A noticeable decrease in V_s near the deformed section was indicated by the HR-SW survey. Therefore, a down-hole PS-logging was carried out to directly measure the profile of V_s with depth. Similarly, RI-logging using the Gamma Ray attenuation technique was performed for profiling the variations of wet density, ρ_t, and the natural water content, w_n, with depth.

Fig. 6 shows the profiles of V_s, N-value, ρ_t, ρ_d and w_n at three locations of BV21-1, BV21-2 and BV21-3, respectively (see Fig.3). As seen in Fig. 3-18, the horizontal layer over the depths roughly from 10m to 13m for the length between BV21-1 and BV21-2 is seemingly soft by showing higher

water content with the relatively low values of V_s, N-value, and ρ_d. The supposed soft soil layer corresponds to the portion characterized by the low-velocity from surface wave survey.

Meanwhile, both of V_s and N-value appear relatively large for the soil layer improved by cement-mixing (i.e., the portions for the first and second remedies, see Fig. 3).

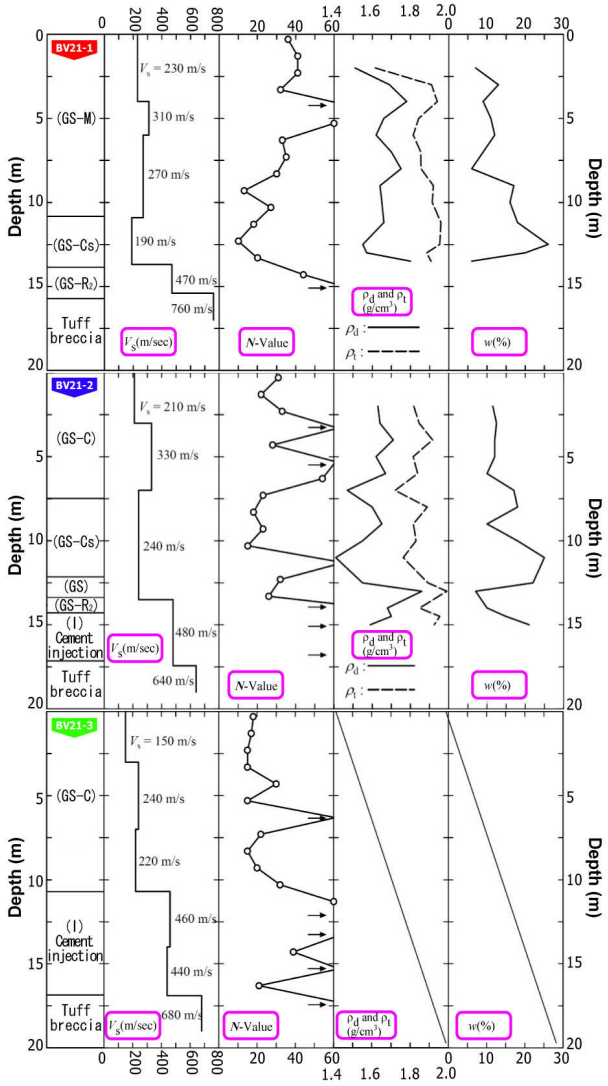

Fig. 6 Profile of physical properties of the fill.

The physical properties, together with the compaction characteristics were measured using disturbed soil samples retrieved at three locations; i.e., the two samples at BH1, BH2 and the other sample at point A on the slope (see Fig. 3).

The soil at BH1 corresponds to the severely damage portion. Similarly, the soil at BH2 represents the fill material on the same level as the soil at BH1.

On the other hand, the soil at point A may well be regarded as a representative sourcing for the fill material. Fig. 7 shows the grain size distribution of these three samples. It is obvious that the soils from BH1 and BH2 are much finer in grain size by showing the fines content, F_c = 49.0% and 40.2% for BH1 and BH2, respectively, whereas F_c = 25.2% at point A.

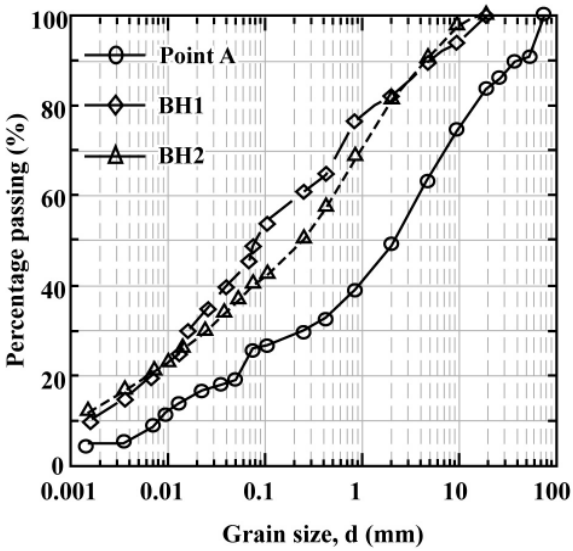

Fig. 7 Grain-size distribution curves.

Fig. 8 shows the compaction curves of two samples at point A and BH2. The maximum dry density, $\rho_{d\ max}$, of the BH2 sample was far smaller than the other sample (n.b., $\rho_{d\ max}$=1.572 g/cm^3 for the BH2 sample and $\rho_{d\ max}$=1.832 g/cm^3 for the other), whereas the optimum water content was higher (n.b., w_{opt}=23.6 % for the BH2 sample and w_{opt}=15.6 % for the other.

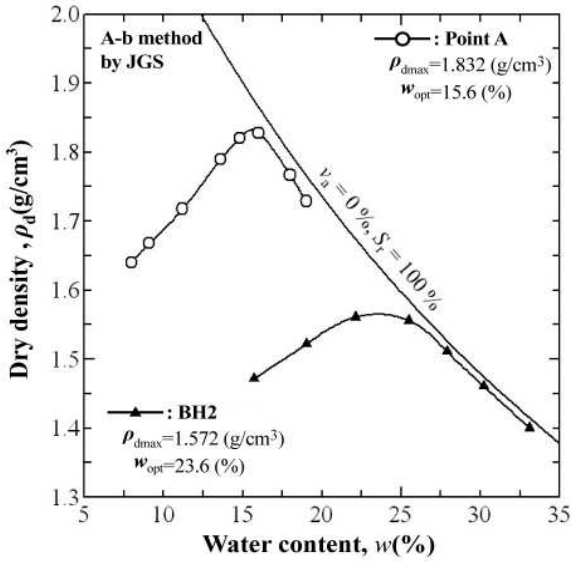

Fig. 8 Compaction curves.

In addition, the controlled value for the density was set to 0.9$\rho_{d\ max}$ based on the compaction curve similar to that of the sample at point A. It is now almost certain that the soft soil layer with larger amount of fines, and having lower values of V_s, N-

value and ρ_d is responsible for the damage of the wall as shown in Fig. 6. The profile of $V_{s,f}$ with depth is shown in Fig. 9, in which the result of the BE test is also shown for comparison.

The $V_{s,lab}$ from the BE test almost coincided with $V_{s,f}$ at the relevant depth when the sustained σ_v of the laboratory sample was 22.5 kPa, noting that the σ_v of 22.5 kPa accounts for merely one-tenth of in-situ overburden pressure at the prescribed depth.

In an attempt to obtain the shear strength at the damaged section, the constant-pressure DST (for the details of apparatus, see Shibuya et al., 2005) was performed. The relationship between the shear stress and the horizontal displacement is shown in Fig. 10, in which similar result of the sample from point A is also shown for comparison.

The maximum shear stress, τ_{max}, of 17 kPa was very small for the sample at the damaged section, bearing the overburden height of the embankment of about 10m in mind. The stress-displacement curve exhibited no peak for the sample, whereas it showed a higher strength involved with a distinct peak for the other sample comprising fewer fines.

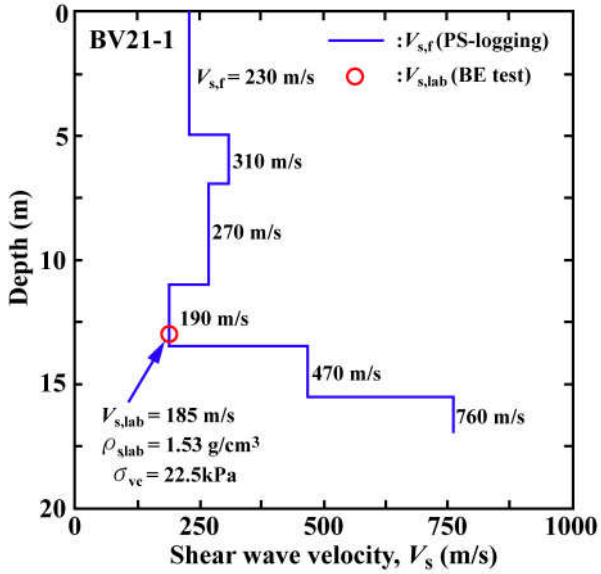

Fig. 9 Results of PS-logging and BE test.

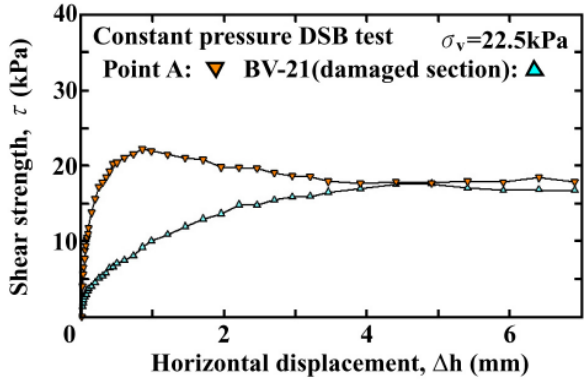

Fig. 10 τ-Δh relationships in constant pressure DST.

According to the results of site investigation performed, the soil at the damaged section is currently saturated (see Fig.5). This means that the initially unsaturated soil at compaction is soaked gradually possibly due to seepage flow into the fill. Soaking test was, therefore, carried out in an attempt to examine the deformation behavior during the process of soaking.

The results of soaking test are shown in Fig.11. In the event of soaking, the sample at the deformed section exhibited a considerable amount of settlement with time to reach the compressive strain of 1.1 % over a period of one day. Conversely, no volume change was observed for the other sample.

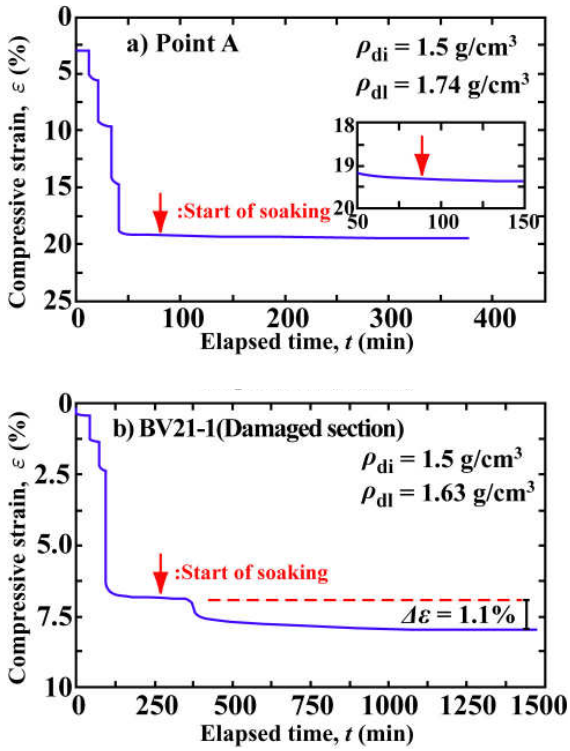

Fig. 11 Results of Soaking test at σ_v = 200kPa.

3 SCENARIO OF WALL DAMAGE

The results of site investigation have revealed the fact that a 3m-thick weak soil layer extends behind the damaged section of the wall. The weak soil layer may be characterized with unexpectedly low values of V_s, ρ_d and the SPT N-value. In addition, the soil properties can be characterized by the occurrence of a considerable amount of settlement on soaking. Fig.12 shows the pictures inside the wall at the deformed section.

A space was found underneath the geotextile, suggesting that the weight of the fill above the geotextile was partially supported by the geotextile. In this paper, the new wording of “hammock state” is conveniently used for describing it.

Based on this observation, the background as well as the mechanical interpretation for the damage of the wall can be postulated as an image shown in Fig.13, it may be described such that;

i) a considerable amount of subsidence took place over the weak soil layer in the lower part of the reinforced earth due to seepage of rainfall water,
ii) the weight of the upper fill was partially supported by the geo-textile hooked on the concrete panels, and
iii) the concrete panels associated with the hammock state were severely damaged by the unexpectedly large downwards compression force triggered by the tension force of the geotextile.

Once the "hammock state" was reached inside the wall, the overburden stress corresponding to the hammock state in the fill will be dramatically reduced, which in turn would bring about decrease of the shear resistance between the geo-textile and the surrounding soil.

The notion is strongly supported by the results of laboratory tests that the estimated σ_v at the deformed section was as small as one-tenth of the supposed σ_v (see Fig. 9) and that the shear strength was far smaller than the supposed value (see Fig.10).

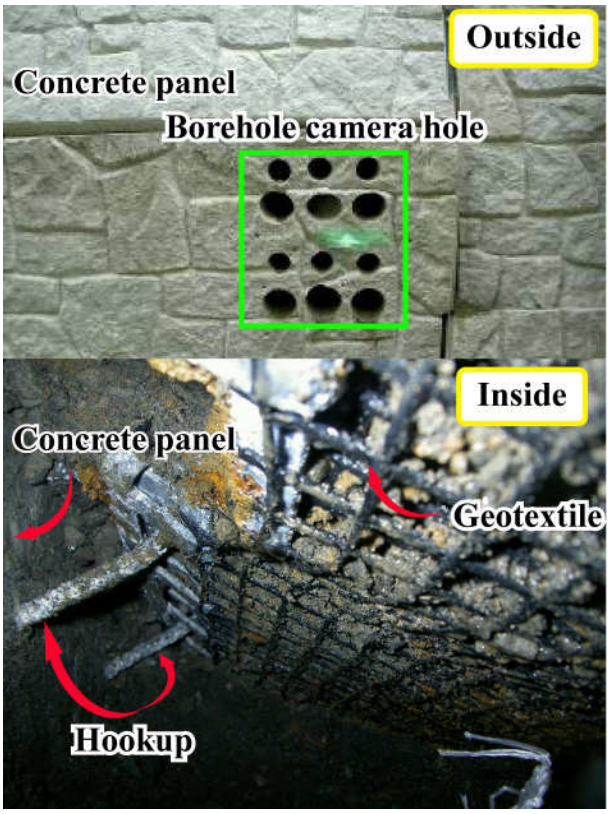

Fig. 12 Pictures inside reinforced earth wall.

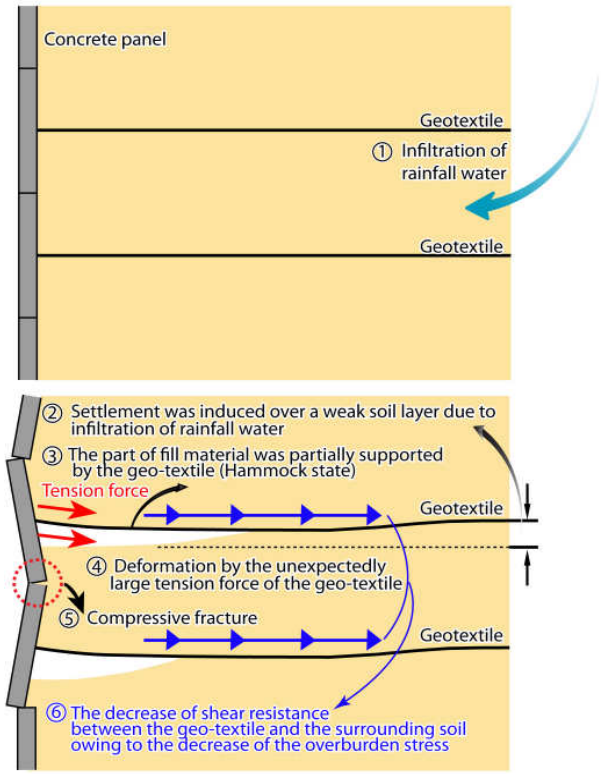

Fig. 13 Mechanical behaviour of a largely-deformed reinforced earth wall with geo-textile.

4 NUMERICAL SIMULATION

Prior to considering countermeasures to re-stabilize the wall, numerical analysis was carried out in order to simulate the development of large deformation that took place on the reinforced earth wall. Since the reinforced earth wall had experienced unexpected deformation of the wall during construction, the wall was re-constructed twice. However, the wall deformation showed no sign to cease even at the final stage of the construction.

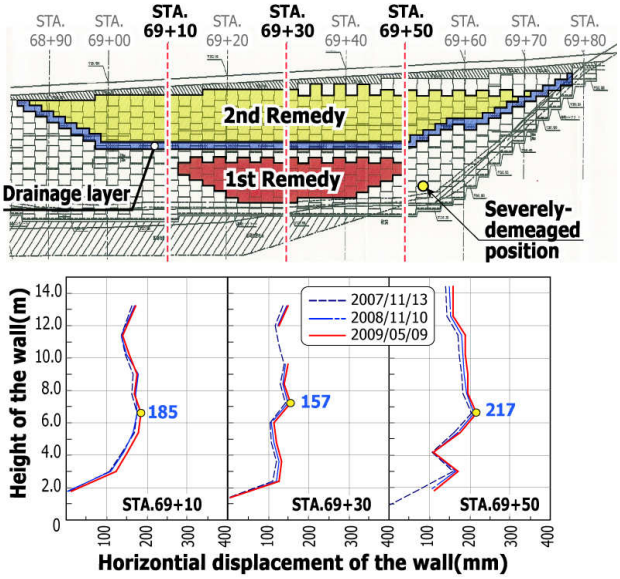

Fig. 14 Observed deformations of the wall facing.

As seen in Fig.14, the range for the maximum value of horizontal deformation was 150 to 200mm. This corresponds to deformation rates of 1.0 to 1.5% against the height of the wall.

Fig.15 shows a representative cross section used in the numerical analysis, Note that the cross section of STA69+50 corresponds to the portion where the wall was severely damaged.

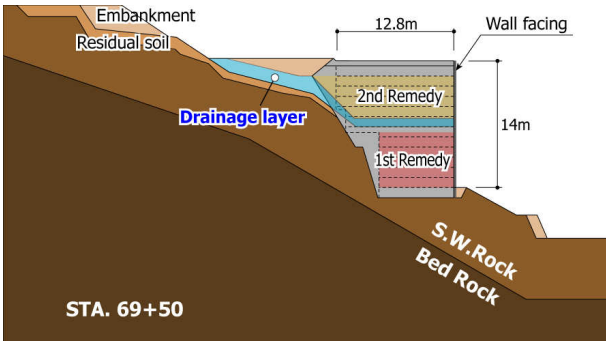

Fig. 15 Cross section used in the numerical analysis

Fig. 16 shows the record of rainfall at the site. It shows that the measured displacement increased after raining. This result may be interpreted due to the effects of infiltration water caused by heavy rains, which remained inside the embankment, despite that the drainage layer was made at the time of the second remedy construction.

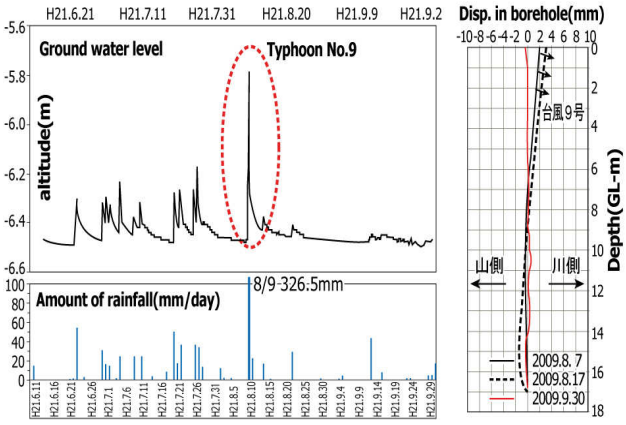

Fig. 16 Record of rainfalls at the site

As shown in Fig.17, the geogrids were modeled using "GEOGRID ELEMENT" of the PLAXIS.

Fig. 18 shows how the reinforced earth wall deforms according to the increase in the ground water level. The maximum amount of displacement with and without raining is 211.5mm and 148.3mm, respectively. This simulation demonstrates that the infiltration water permeating the reinforced earth wall has a strong influence on the movement of the wall.

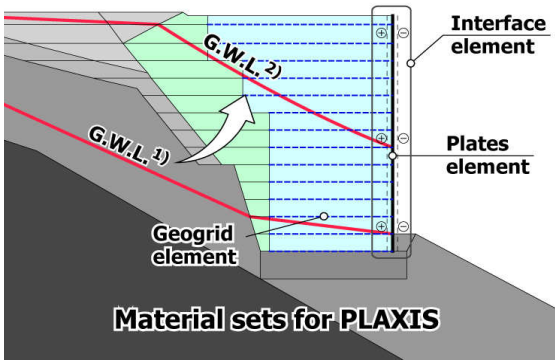

Fig. 17 Seepage analysis by PLAXIS

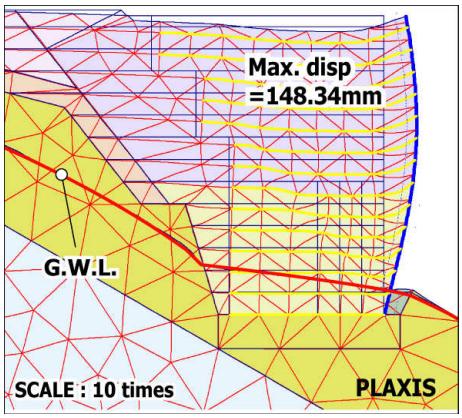

(a)

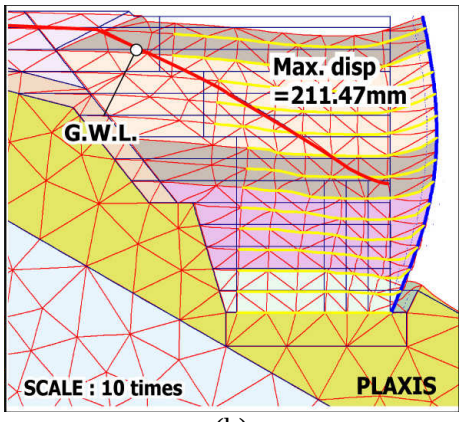

(b)

Fig. 18 Deformed meshes due to increase in water level.

Fig. 19 shows the results of analysis performed for two cases, i.e., the case of normal geogrid and the other case of geogrid subjected to the condition of "hammock". Based on the observation, the hammock condition was assumed over the lower part of the wall comprising the soft soil layer. The effect of hammock was significant in that large deformation was observed near the wall by showing the maximum shear strain increment almost ten times the normal condition.

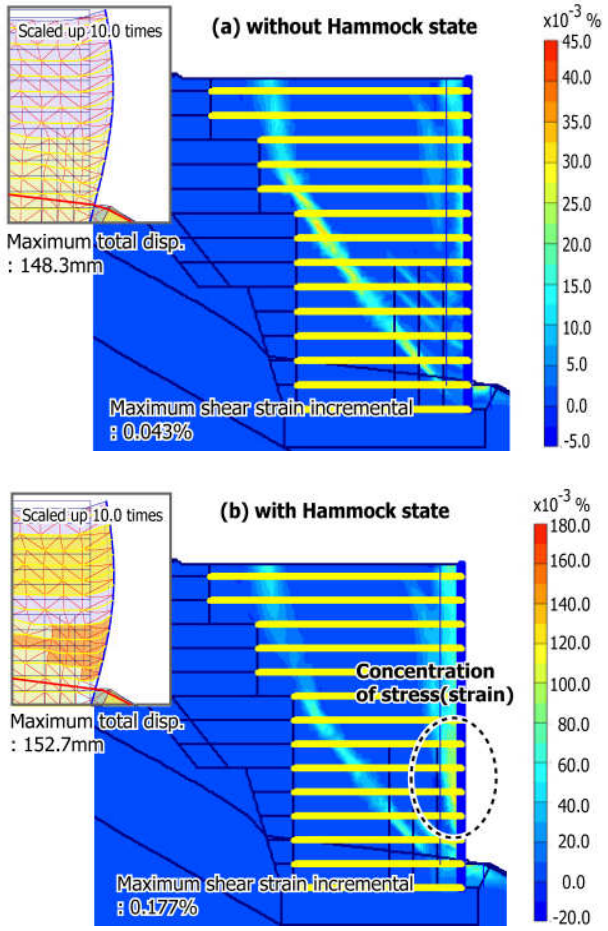

Fig. 19 Incremental shear strains in the fill, together with the deformed meshes near the wall facing.

As depicted in Fig.20, the large deformation of the wall may be induced with the sequence of events in the following. First, highly compressive filling materials existed inside the backfill. Second, rainwater and the water in a valley infiltrated into the layers, which in turn induced deformation in compression.

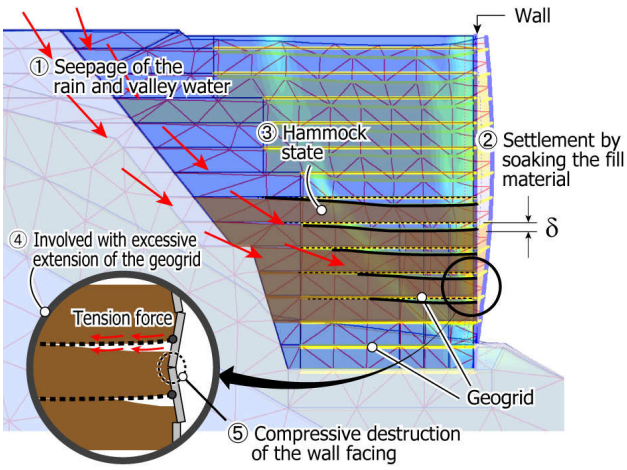

Fig. 20 Sequence for the development of wall.

As a result of the generation of settlement in the weak soil layer, so-called 'hammock state', in which the weight of the upper filling was partially supported by the geogrids, was gradually formed.

This condition generated high tensile force to the geogrids, which in turn induced stress concentration on the concrete panel connected to the high-tensioned geogrids. As a consequence, a type of compression failure took place on the concrete panels.

5 COUNTERMEASURES

Fig.21 shows the overall scheme of countermeasures employed. Based on the results of site investigation, together with numerical simulation, it was needed to prevent any seepage water from infiltrating into the embankment so that geosynthetic drain was first installed as an urgent, and hopefully permanent, remedial work.

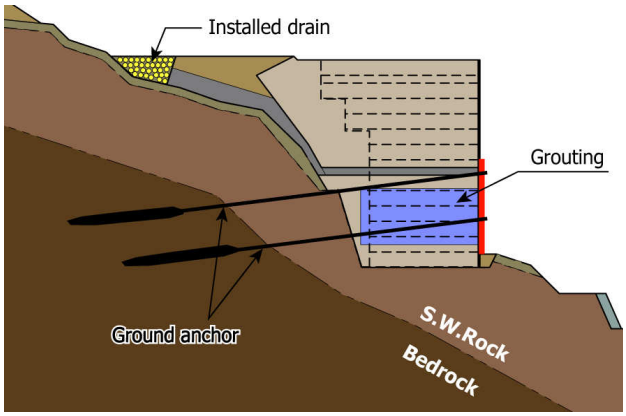

Fig. 21 Scheme of countermeasures employed.

Fig.22 shows the implementation of the geosynthetic drain with gravels. As seen in Fig.23, the drain system was highly effective in respect that a considerable amount of seepage water from a small valley behind was discharged over a substantially long period after each rainfall.

Second, cement-grouting was implemented for preventing further development of compression of the soft soil layer, hence to avoid further damage to the wall facing.

Eventually, ground anchors were planted in order to enhance the overall stability of the wall. The minimum rate for the safety factor, F_s, was 1.51 after implementing the ground anchors, the value of which exceeded F_s =1.25 of the allowable rate for the safety factor in design.

Fig.24 shows the picture after the remedial work. In April 2010, the wall was successfully open to the public service.

Fig. 22 Implementation of geosynthetic drain.

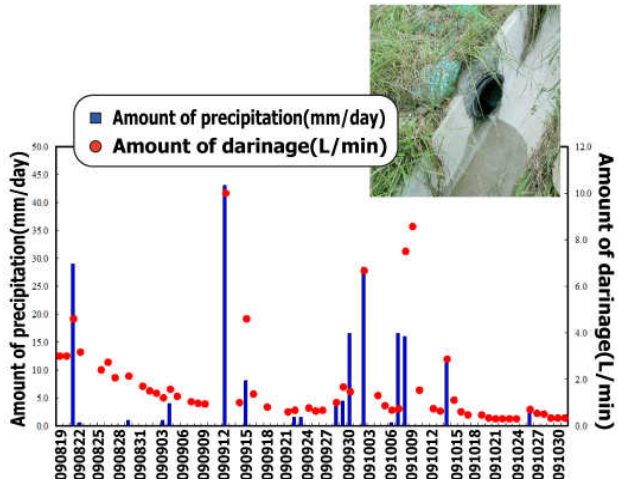

Fig. 23 Discharge of water from geosynthetic drain.

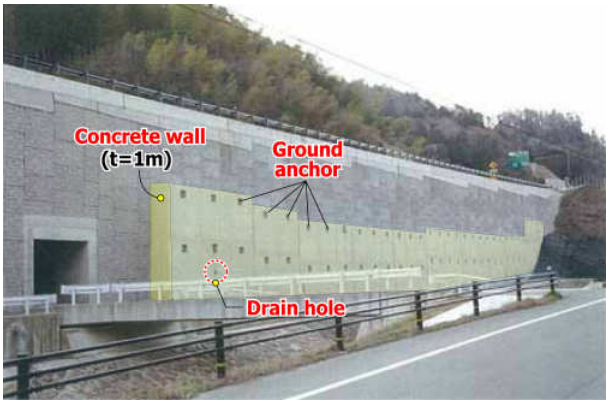

Fig. 24 The wall open to service (April 2010).

6 CONCLUSION

In this case study, the wall damage was seemingly induced in association with successive development of compressive strain of 3m-thick weak soil layer at the lower part of the fill. The soil comprised larger amount of fines, and hence it was initially hard to compact.

A scenario for the wall damage may be described such that a considerable amount of subsidence took place over the weak soil layer due to seepage of rainfall water, the weight of the upper fill was partially supported by the geo-textile hooked on the concrete panels, and the concrete panels associated with this “hammock state” were severely damaged by the unexpectedly large downwards compression force triggered by the tension force of the geotextile.

Bearing this scenario in mind, the following may be pointed out:

i) When the wall was constructed using fine-grained local soils, care should be taken for the variation of the soil properties such as the grain-size distribution, the characteristics of compaction, stiffness, strength *etc*. These properties should frequently be examined in the laboratory, and the results should be properly considered for the scheme for the wall construction. Geotechnical engineers should be brave enough for disposing the local soil that is not suitable for the compaction work.

ii) In the reinforced earth with concrete facing, the state of under-compaction is likely to take place for the portion adjacent to the wall. Extra care should be taken for a thorough management of compaction work adjacent to the wall, in particular. Otherwise, a better geomaterial such as gravels may preferably be used.

iii) A performance-based design should be implemented urgently in the design manual. If the deformation analysis considering the seepage water into account was performed prior to construction, the trouble encountered in this case study could have been avoided.

iv) The countermeasures employed in this case study, i.e., the geosynthetic drain system to prevent any seepage water from infiltrating into the embankment, cement-grouting for reducing further development of compression of the soft soil layer and ground anchors to enhance the overall stability of the wall, all worked well. The effects of the countermeasures to control displacements of the wall and the extensional strain of the geo-textile were successfully confirmed by 2D and 3D numerical analysis.

v) The importance of co-operation between wall engineers and geotechnical engineers was again acknowledged in this case study.

REFERENCES

Bathurst, R.J., Hatami, K. (2006): "Parametric analysis of reinforced soil walls with different height and reinforcement stiffness", Geosynthetics, J. Kuwano & J. Koseki. Pp.1343~ 1346

Chirica, A., Baicu, A.M. (2006): "Some considerations about the calculus of earth retaining structures reinforced with geosynthectics", Geosynthetics, J. Kuwano & J. Koseki. Pp.1271~1274

Design Codes for Concrete Structures of Japan Railway, (1992): Japan Ministry of Transportation, ISBN 4-621-03760-9 C3051, Maruzen Print Co. Ltd.,.79-107 (in Japanese)

Moraci, N., Rimoldi,P., Mandaglio,M.C. (2006): "A design procedure for geosynthetic reinforced soil structures", Geosynthetics, J. Kuwano & J. Koseki. Pp.1249~1254

Queiroz, P.I.B., Gomes, R.C. (2006): "Numerical tools for geosynnthetic reinforced walls design: A performance assessment on the basis of laboratory-scale models results", Geosynthetics, J. Kuwano & J. Koseki. Pp.1335~1338

Shibuya, S. , Kawaguchi, T. and Chae, J-G. (2007): "Failure of Reinforced Earth wall as attacked by Typhoon No. 23 in 2004", Soils and Foundations, Vol.46, No.2, pp.153-160

Shibuya, S., Koseki, J. and Kawaguchi, T. (2005): "Recent developments in deformation and strength testing of geomaterials", Keynote Lecture, Deformation Characteristics of Geomaterials -Recent Investigations and Prospects (Di Benedetto H. et al edns), Taylor Francis Group London, pp.3-28

Tatsuoka,F., Tateyama, M., Tamura, Y. and Yamauchi. H. (2000): "Lessons from the failure of full-scale models and recent geosynthetic-reinforced soil retaining wall", Proc. the second Asian Geosynthetics Conference, GeoAsia 2000, Kuala Lumpur, Vol.1, pp.23-53

Tatsuoka,F., Tateyama, M., Tamura, Y. and Yamauchi. H. (1997): "Geosynthetic-reinforced soil retaining walls as important permanent structures", 1996-1997 Mercer Lecture, Geosynthetic International, Vol.4, No.2, pp.21-136